LA-UR- 96 - 0073

Title: A UNIFIED VIEW OF COHERENT AND INCOHERENT DIHYDROGEN EXCHANGE IN TRANSITION METAL HYDRIDES BY NUCLEAR RESONANCE AND INELASTIC NEUTRON SCATTERING

Author(s): H. H. Limbach, S. Ulrich, G. Buntkowsky, S. Sabo-Etienne, B. Chaudret, G. J. Kubas, J. Eckert

Submitted to: Berichte der Bunsengesellschaft fur Physikalische Chemie

Los Alamos
NATIONAL LABORATORY

MASTER

A Unified View of Coherent and Incoherent Dihydrogen Exchange in Transition Metal Hydrides by Nuclear Magnetic Resonance and Inelastic Neutron Scattering

H.H.Limbach,[a] S.Ulrich,[a] G.Buntkowsky,[a] S.Sabo-Etienne,[b] B.Chaudret,[b] G.J.Kubas,[c] J.Eckert[c]

a: Institut für Organische Chemie der Freien Universität Berlin, Takustr. 3, D-14195 Berlin Germany, FAX (49)30-8385310, email: limbach@chemie.fu-berlin.de

b: Laboratoire de Chimie de Coordination du CNRS (UP 8241), 205, route de Narbonne, F-31077 Toulouse-Cedex, France, email: chaudret@lcctoul.lcc-toulouse.fr

c: LANSCE, Los Alamos National Laboratory, Los Alamos,Masil Stop H805, NM87545, USA, email: juergen@beta.lanl.gov

In this paper a unified view of coherent and incoherent dihydrogen exchange in transition metal hydrides by nuclear magnetic resonance (NMR) and inelastic neutron scattering (INS) is presented. It is shown that both exchange processes coexist i.e. do not transform into each other although they may dominate the spectra in different temperature ranges. This superposition is the consequence of the incorporation of the tunnel frequency J of the coherent process into the nuclear two-spin hamiltonian of hydrogen pairs which allows to treat the problem using the well known density matrix theory of NMR

line—shapes developped by Alexander and Binsch. It is shown that this theory can also be used to predict the line—shapes of the rotational tunneling transitions observed in the INS spectra of transition metal dihydrogen complexes and that both NMR and INS spectra depend on similar parameters. In particular, two simple models of dihydrogen exchange effects on the NMR and INS spectra are discussed. In the first model a single site—two—spin system is considered involving four nuclear spin levels, characterized by the average tunnel frequency J and the rate constant k of incoherent dihydrogen exchange. Whereas J leads to the usual NMR line—splitting the increase of k induces line—broadening and coalescence into a single line by averaging of the chemical shifts of the two hydrogen atoms. By contrast, the quantum coherences between the nuclear singlet and triplet states which are not observable by NMR but seen in INS as rotational tunneling transitions are predicted to decay with $2k$ leading to an homogeneous broadening of $2k/\pi$ of the corresponding INS bands. This result explains the disappearance of these bands when temperature is raised as k increases monotonously with the latter. Since in practice many sites have to be taken into account, corresponding to different molecular configurations, conformations, solvent environments, or simply different rovibrational states, this one—site model is only valid in the case of rapid interconversion of the different sites. The effects on this interconversion without and with a combined dihydrogen permutation on the NMR and INS spectra is studied in a two—site model, adapted to typical experimental situations encountered in NMR and INS. The results obtained are then illustrated using experimental examples from both spectroscopies. Finally, a physical interpretation of the loss of quantum coherence between the triplet and singlet states by the incoherent exchange is proposed, associated to sudden dihydrogen rotations either via incoherent tunneling or via a free over—barrier rotation which inverts the rotational wave functions of $o-H_2$ but not of $p-H_2$ states. The incoherent tunnel process can explain experimental findings by INS of a non—Arrhenius behavior of the rate constant of the incoherent process in the case of dihydrogen complexes exhibiting a low barrier for dihydrogen rotation. The absence of kinetic HH/HD isotope effects found by NMR for cases with high barriers seems then to indicate a heavy atom motion, e.g. a ligand reorientation in the rate limiting step of the incoherent rotation.

1. Introduction

For a long time, the dynamics of hydrogen exchange reactions, e.g. ammonium and methyl group rotations in molecular solids have been studied both by inelastic neutron scattering (INS)[1] and nuclear magnetic resonance (NMR)[2] techniques. At cryogenic temperatures, the exchange is generally coherent, i.e. characterized by a tunnel frequency ν_t which is directly observable as a tunneling transition in the INS spectra. At higher temperatures, a transition into an incoherent exchange regime occurs characterized by typical line–shifts towards the elastic line and line–broadening, eventually leading to a very broad inelastic line disappearing at high temperatures. On the other hand, both coherent and incoherent group rotations also give rise to characteristic NMR spectra and NMR relaxation [2].

Recently, it has been shown by Kubas et al. [3] that dihydrogen can be coordinated in side–on configuration to transition metals. Moreover, it was found by INS that the dihydrogen group in these compounds is also subject to coherent rotational tunneling. On the other hand, in recent years several authors have observed unusually large (Hz to kHz) non–magnetic "exchange couplings" between metal bound protons of transition metal trihydrides [4–6] and dihydrides [7] dissolved in organic liquids which strongly increased with temperature up to a point where a "classical" or incoherent dihydrogen exchange sets in. These "exchange" couplings J_{exch} were identified by Zilm [5a–d] et al. and Weitekamp [5f] with the average frequency $\bar{\nu}_t$ of coherent dihydrogen exchange tunneling. This phenomenon has aroused a wide experimental and theoretical interest [5–7]. One main consequence of these observations was the possibility to include the tunnel frequency in the usual high–resolution nuclear two–spin hamiltonian [8], i.e.

$$\mathcal{H} = \nu_1 \hat{I}_{z1} + \nu_2 \hat{I}_{z2} + J \hat{I}_1 \hat{I}_2, \tag{1}$$

where ν_i represent the chemical shifts, $\hat{I}_{zi}$ and $\hat{I}_i$ the usual spin operators, and J the apparent coupling constant corresponding to the sum [5]

$$J = J_{exch} + J_{magn}. \tag{2}$$

J_{magn} is the usual scalar magnetic coupling constant. Since we are concerned in this paper mainly with the case $J_{exch} \gg J_{magn}$ we will drop the subscript in Eq. (2) and set $J \approx$

J_{exch} throughout this paper.

This incorporation of coherent tunneling into the nuclear spin hamiltonian has some consequences which have not yet been fully recognized to our knowledge. The main consequence is that the transition from the coherent to the incoherent dihydrogen exchange regime does not mean that one phenomenon excludes the other but that both coexist in the whole temperature range; the apparent transition is only a consequence of the different temperature dependence of the parameters describing both phenomena. This conclusion immediately follows from the well established NMR line—shape theory devised by Alexander and Binsch [9] which has been very often used in order to describe the NMR line—shapes of J — coupled spin systems in the presence of incoherent or "chemical" exchange processes. Here we use this theory to describe the NMR spectra of superposed coherent and incoherent dihydrogen exchange of transition metal hydrides which reveals insight into the physical meaning of the superposition of both processes.

Another consequence of Eq. (1) is also addressed in this paper, namely to show that the Alexander—Binsch theory does not only give a consistent description of the NMR but also of the INS line—shapes of transition metal hydrides which are not yet well understood up to date. Thus, it becomes possible to discuss the results of both methods within a common theoretical framework in terms of a simple phenomenological exchange model.

In the following theoretical section we will shortly review the Alexander—Binsch theory and then discuss the example of a one—site—four—level system of dihydrogen exchange. This model will then be expanded to a two—site—eight—level system but it will be shown that the latter and even a multi—site system reduces, under certain circumstances, to the one—site system. These models will then be applied to discuss experimental NMR and INS spectra of some transition metal hydrides subject to coherent and incoherent dihydrogen exchange.

2. Theoretical Section

2.1. The Alexander–Binsch formalism

Within the framework of the Alexander–Binsch formalism, the NMR spectra of exchanging spin systems in sites r, s, t... are calculated by solving the equation of motion of the complex density matrix ρ of an ensemble of nuclear spins of interest in composite Liouville space [9b]

$$\frac{d\rho}{dt} = (-i\mathcal{L} + X + \mathcal{R})\rho, \quad \rho_{mn} = <m|\rho|n>. \qquad (3)$$

All quantities in Eq. (3) are well–known. The diagonal elements of ρ correspond to populations and the off–diagonal elements $\rho_{\kappa\lambda} = \rho^*_{\lambda\kappa}$ to quantum coherences. $\mathcal{L}$ is the Liouville operator depending only on the nuclear spin Hamiltonian $\mathcal{H}$, i.e.

$$\mathcal{L}_{\mu_r\nu_r,\kappa_s\lambda_s} = \delta_{rs}(\mathcal{H}_{\mu\kappa}\delta_{\lambda\nu} - \mathcal{H}_{\lambda\nu}\delta_{\mu\kappa}). \qquad (4)$$

δ represents the Kronecker symbol, μ_r etc. the nuclear spin functions of the environment r; generally, the usual product spin functions are used as basis. The subscripts r are employed only when necessary; since $\mathcal{L}$ has a block–diagonal structure for each spin system, they can be omitted on the right side of Eq. (4). $\mathcal{R}$ is the Redfield relaxation operator describing the interaction with the bath; in order to evaluate $\mathcal{R}$ a specific relaxation mechanism must be chosen, e.g. a dipole–dipole relaxation mechanism. However, in usual NMR line–shape calculations $\mathcal{R}$ is generally assumed to be diagonal, and all diagonal elements are given by $-1/T_2 = -\pi W_0$, where T_2 is the effective transverse relaxation time and W_0 the corresponding line–width in the absence of exchange. X represents the operator describing all chemical exchange processes. For intramolecular exchange processes between different sites the elements of X are given in composite Liouville space of the exchanging by [9b,9c]

$$X_{\mu_r\nu_r,\kappa_s\lambda_s} = \delta_{\mu_r\kappa_r}\delta_{\nu_r\lambda_r}[\,\delta_{rs}\sum_{t\neq r} k_{rt} + (1-\delta_{rs})k_{rs}]. \qquad (5)$$

k_{rs} is the rate constant of the interconversion between r and s. For intramolecular mutual exchange processes between two nuclei i and j within a given subspace r involving the rate constant k_{rr}^{ij} the elements of X are given by [9b,9c]

$$X_{\mu_r\nu_r,\kappa_r\lambda_r} = -\sum_{i<j}\sum k_{rr}^{ij}\delta_{\mu_r\kappa_r}\delta_{\nu_r\lambda_r} + k_{rr}^{ij}P_{\mu_r\kappa_r}^{ij}P_{\nu_r\lambda_r}^{ij}. \qquad (6)$$

P^{ij} is the permutation operator exchanging i and j, and its elements $P_{\mu_r\kappa_r}^{ij} = 1$ if μ_r and ν_r

differ only by the permutation of the spins i and j, otherwise it is zero. We note that Eq. (5) is independent of the basis, but Eq. (6) is formulated in the product spin basis and has to be transformed when another basis is used.

The NMR spectra can easily be calculated from the expectation values of the usual lowering or raising operators according to the equation

$$< \Gamma > = I\rho \tag{7}$$

formulated in Liouville–space, where only single quantum coherences are important. After Fourier transformation, they immediatedly give the contribution of the particular transition to the NMR spectrum. Therefore, for line–shape calculations Eq. (3) must be set up and solved only for the the single quantum coherences, if they are created in a one–pulse NMR experiment. We note that all parameters contained in Eqs. (3 − 6) are phenomenological and obtained by comparison of experimental and numerically calculated line–shapes.

As will be proposed below, the formalism may also be used in order to calculate the INS rotational tunneling transitions for proton pairs, where attention has to be paid to the different selection rules in this kind of spectroscopy.

2.2. A one–site–four–level tunneling model of dihydrogen exchange

In the first step we consider the simplest dihydrogen exchange tunneling model involving a single proton pair in a single site leading to four nuclear spin levels. The nuclear spin hamiltonian is given by Eq. (1), i.e. characterized by two chemical shifts ν_1 and ν_2 and a single tunnel splitting J corresponding to a single pair of coherent tunnel states outside the magnetic field. In addition, we consider an incoherent mutual exchange between the two protons characterized by the rate constant k. In the product spin basis the four nuclear spin functions are given by $1 \equiv \alpha\alpha$, $2 \equiv \alpha\beta$, $3 \equiv \beta\alpha$ and $4 \equiv \beta\beta$. As shown in the Appendix, these functions are in agreement with the Pauli exclusion principle. Neglecting relaxation, it follows from the previous section that the time evolution of the populations and of the zero quantum coherences is given by the following equations

$$\frac{d\rho_{11}}{dt} = \frac{d\rho_{44}}{dt} = 0, \tag{8}$$

$$\frac{d\rho_{22}}{dt} = -k\rho_{22} - i\pi J\rho_{23} + i\pi J\rho_{32} + k\rho_{33}, \tag{9}$$

$$\frac{d\rho_{23}}{dt} = -i\pi J\rho_{22} + [-k + 2\pi i(\nu_2 - \nu_1)]\rho_{23} + k\rho_{32} + i\pi J\rho_{33}, \tag{10}$$

$$\frac{d\rho_{33}}{dt} = k\rho_{22} + i\pi J\rho_{23} - i\pi J\rho_{32} - k\rho_{33}, \tag{11}$$

of the single quantum coherences by

$$\frac{d\rho_{12}}{dt} = [-k\frac{1}{T_2} + 2\pi i(\nu_2 + J/2)]\rho_{12} + [k - i\pi J]\rho_{13}, \tag{12}$$

$$\frac{d\rho_{13}}{dt} = [-k\frac{1}{T_2} + 2\pi i(\nu_1 + J/2)]\rho_{13} + [k - i\pi J]\rho_{12}, \tag{13}$$

$$\frac{d\rho_{24}}{dt} = [-k\frac{1}{T_2} + 2\pi i(\nu_1 - J/2)]\rho_{24} + [k + i\pi J]\rho_{34}, \tag{14}$$

$$\frac{d\rho_{34}}{dt} = [-k\frac{1}{T_2} + 2\pi i(\nu_2 - J/2)]\rho_{34} + [k + i\pi J]\rho_{24}. \tag{15}$$

and of the double quantum coherences by

$$\frac{d\rho_{14}}{dt} = [-\frac{1}{T_2} + 4\pi i\nu_2]\rho_{14}, \tag{16}$$

It is helpful to transform the above equations into the basis of the symmetrized spin functions, i.e. the nuclear triplet states and the singlet state

$$1 = \alpha\alpha = T_1, \, 2 = T_0 = (\frac{1}{\sqrt{2}}(\alpha\beta + \beta\alpha), \, 4 = T_{-1} = \beta\beta, \, 3 = S = \frac{1}{\sqrt{2}}(\alpha\beta - \beta\alpha). \tag{17}$$

The density matrix σ in this basis can easily be evaluated and we obtain

$$\frac{d\sigma_{11}}{dt} = \frac{d\sigma_{22}}{dt} = \frac{d\sigma_{33}}{dt} = \frac{d\sigma_{44}}{dt} = 0, \tag{18}$$

$$\frac{d\sigma_{23}}{dt} = [-2k + 2i\pi J]\sigma_{23}, \tag{19}$$

$$\frac{d\sigma_{12}}{dt} = \pi i(\nu_1 + \nu_2)\sigma_{12} + \pi i(\nu_1 - \nu_2)\sigma_{13}, \tag{20}$$

$$\frac{d\sigma_{13}}{dt} = \pi i(\nu_1 - \nu_2)\sigma_{12} + [-2k + \pi i(\nu_1 + \nu_2) + 2\pi i J]\sigma_{13}, \tag{21}$$

$$\frac{d\sigma_{24}}{dt} = \pi i(\nu_1+\nu_2)\sigma_{24} + \pi i(\nu_1-\nu_2)\sigma_{34}, \tag{22}$$

$$\frac{d\sigma_{34}}{dt} = \pi i(\nu_1-\nu_2)\sigma_{24} + [-2k+\pi i(\nu_1+\nu_2)+2\pi i J]\sigma_{13}. \tag{23}$$

Outside the magnetic field all Larmorfrequencies are zero and one obtains

$$\frac{d\sigma_{11}}{dt} = \frac{d\sigma_{22}}{dt} = \frac{d\sigma_{33}}{dt} = \frac{d\sigma_{44}}{dt} = \frac{d\sigma_{12}}{dt} = \frac{d\sigma_{24}}{dt} = 0, \tag{24}$$

$$\frac{d\sigma_{23}}{dt} = [-2k+2i\pi J]\sigma_{23}, \quad \frac{d\sigma_{32}}{dt} = [-2k+2i\pi J]\sigma_{32}, \tag{25}$$

$$\frac{d\sigma_{13}}{dt} = [-2k+2\pi i J]\sigma_{13}, \quad \frac{d\sigma_{34}}{dt} = [-2k+2\pi i J]\sigma_{13} \tag{26}$$

Let us now discuss Eq. (18 − 23) in more detail. The situation where $k \approx 0$ is illustrated schematically in Fig. 1. If $J << |\nu_1-\nu_2|$ and ν_0, the spectrometer frequency, the energy level diagram of Fig. 1a results. The potential functions for the dihydrogen exchange are included schematically, where the barrier height is in reality much larger than indicated. The states $\alpha\alpha$ and $\beta\beta$ are delocalized and associated with the upper tunneling state via the Pauli exclusion principle. The states $2 = \alpha\beta$ and $3 = \beta\alpha$ are localized pocket states of different energy because of the condition $J << |\nu_1-\nu_2|$. Therefore, the observable transitions ν_{31} and ν_{42} indicated in Fig. 1a are split by the total coupling constant J as usual. The same is true for the observable transitions ν_{21} and ν_{43}.

In the case where the exchange coupling constant $J >> |\nu_1-\nu_2|$ but $J << \nu_0$ the level diagram of Fig. 1b is obtained. In NMR, only the transitions within the triplet states are allowed but not between the singlet and the triplet states. Therefore, only a single line is observed by NMR at $(\nu_1+\nu_2)/2$ as indicated at the bottom of Fig. 1b. In the absence of a magnetic field $\nu_0 = 0$ and the diagram of Fig. 1c results. All triplet states are degenerate for the hamiltonian of Eq. (1) and coincide into the state T where the subscripts are now omitted. Under these conditions NMR cannot be observed; however, the transitions between singlet and triplet states are allowed in INS; the transition $\nu_{ST} = -J$ appears on the energy loss side of the elastic line situated at the origin and the transition $\nu_{TS} = +J$ on the energy gain side as indicated schematically in Fig. 1c.

The influence of an increase of the rate constant k of incoherent exchange on the NMR spectra calculated from Eqs. (20 − 23) is illustrated in Fig. 2 using arbitrary parameters. In the cases of Fig. 2a ($J = 0$) and 2b ($J << |\nu_1-\nu_2|$) the increase of k firstly leads to line–broadening given by k/π, then coalescence into a single peak which then sharpens. The incoherent exchange can be visualized as interconversion between the well defined pocket states $\alpha\beta$ and $\beta\alpha$ in Fig.1a, or more exactly as the interconversion between the single quantum coherences connected with the states $\alpha\beta$ and $\beta\alpha$. This incoherent exchange renders, therefore, the two protons magnetically equivalent i.e. averages their chemical shifts and possible magnetic couplings to other nuclei, in contrast to the coherent quantum exchange. In Fig. 2c $J \approx |\nu_1-\nu_2|$ leads to the well–known decrease of the signal intensity of the outer transitions ν_{31} and ν_{43}. Now, increasing k still leads to some spectral changes and line–coalescence. By contrast, no line–shape changes occur any more when $J >> \nu_1-\nu_2$ as depicted in Fig. 2d; in other words, the transitions within the triplet sublevels of Fig. 1b are no longer affected by k. Since all states are now delocalized by coherent tunneling, what is then the meaning of k in this regime realized always in the absence of a magnetic field?

This question can easily be answered by a look at the density matrix elements corresponding to the quantum coherences between the S– and T–states given by Eqs. (20 − 26) in the symmetrized spin basis set. These coherences decay − even in the absence of a magnetic field with the rate constant $2k$, leading to a linewidth of $2k/\pi$ of the transitions ν_{ST} and ν_{TS}. The calculated line–shapes of the latter which should be observable in INS are depicted in Fig. 1e. Since k increases monotonously with temperature this simple model, therefore, predicts the INS transitons to broaden monotonously with temperature until they disappear.

2.3. A two–site–eight–level tunneling model of dihydrogen exchange

The above exchange model does not explicitly take into account the inter-conversion between a a multitude of thermally accessible state pairs, populated according to a Boltzmann distribution, and characterized by different nuclear spin hamiltonians,

especially different tunnel splittings. In order to obtain further insight into the way how this interconversion affects the NMR and INS line–shapes we consider in this section a dihydrogen exchange model consisting of two interconverting sites A and B, consisting each of a four–level two–spin system characterized by different exchange coupling constants and chemical shifts. The reaction network considered is illustrated in Fig. 3. The sites may be identified either with different chemical species such as a dihydride configuration and a dihydrogen configuration as indicated, but could also represent different solvent configurations, conformations or simply the rovibrational groundstate and an excited state.

A and B are characterized by the populations x_A and x_B and interconvert with the forward and backward rate constants k_{AB} and k_{BA}, where the equilibrium constant is given by $K = x_B/x_A = k_{AB}/k_{BA}$. The exchange couplings are J^A and J^B. In order to describe the incoherent dihydrogen exchange the states A' and B' have to be included in Fig.3. The corresponding rate constants are k_{AA} and k_{BB}, where we assume in the following that $k_{AA} \ll k_{BB}$ Figs. 3a and 3b differ in the probability p of a dihydrogen permutation associated to the A $\rightleftharpoons$ B interconversion. In Fig.3a $p = 0$ and in Fig. 3b $p = 1/2$. Both networks can, therefore, be combined into a single network.

For this model we obtain the following set of coupled equations for the single quantum coherences

$$
\frac{d}{dt}
\begin{pmatrix} \rho^A_{12} \\ \rho^A_{13} \\ \rho^B_{12} \\ \rho^B_{13} \end{pmatrix}
=
\begin{pmatrix}
-k_{AB}-k_{AA}-1/T_2 +2\pi i(\nu^A_2 +J^A/2) & k_{AA} -\pi i J^A & k_{BA}(1-p) & k_{BA}p \\
k_{AA} -\pi i J^A & -k_{AB}-k_{AA}-1/T_2 +2\pi i(\nu^A_1 +J^A/2) & k_{BA}p & k_{BA}(1-p) \\
k_{AB}(1-p) & k_{AB}p & -k_{BA}-k_{BB}-1/T_2 +2\pi i(\nu^B_2 +J^B/2) & k_{BB} -\pi i J^B \\
k_{AB}p & k_{AB}(1-p) & k_{BB} -\pi i J^B & -k_{BA}-k_{BB}-1/T_2 +2\pi i(\nu^B_1 +J^B/2)
\end{pmatrix}
\begin{pmatrix} \rho^A_{12} \\ \rho^A_{13} \\ \rho^B_{12} \\ \rho^B_{13} \end{pmatrix}
\tag{27}
$$

$$\frac{d}{dt}\begin{vmatrix}\rho_{24}^A\\\rho_{34}^A\\\rho_{24}^B\\\rho_{34}^B\end{vmatrix}=\begin{vmatrix}-k_{AB}-k_{AA}-1/T_2+2\pi i(\nu_2^A-J^A/2) & k_{AA}\ \pi iJ^A & k_{BA}(1-p) & k_{BA}p\\ k_{AA}\ \pi iJ^A & -k_{AB}-k_{AA}-1/T_2+2\pi i(\nu_1^A-J^A/2) & k_{BA}p & k_{BA}(1-p)\\ k_{AB}(1-p) & k_{AB}p & -k_{BA}-k_{BB}-1/T_2+2\pi i(\nu_2^B-J^B/2) & k_{BB}\ \pi iJ^B\\ k_{AB}p & k_{AB}(1-p) & k_{BB}\ \pi iJ^B & -k_{BA}-k_{BB}-1/T_2+2\pi i(\nu_1^B-J^B/2)\end{vmatrix}\begin{vmatrix}\rho_{24}^A\\\rho_{34}^A\\\rho_{24}^B\\\rho_{34}^B\end{vmatrix} \quad (28)$$

In the symmetrized basis for form B we obtain

$$\frac{d}{dt}\begin{vmatrix}\rho_{12}^A\\\rho_{13}^A\\\sigma_{12}^B\\\sigma_{13}^B\end{vmatrix}=\begin{vmatrix}-k_{AB}-k_{AA}-1/T_2+2\pi i(\nu_2^A+J^A/2) & k_{AA}\ -\pi iJ^A & k_{BA}/\sqrt2 & (1-2p)k_{BA}/\sqrt2\\ k_{AA}\ -\pi iJ^A & -k_{AB}-k_{AA}-1/T_2+2\pi i(\nu_1^A+J^A/2) & k_{BA}/\sqrt2 & -(1-2p)k_{BA}/\sqrt2\\ k_{AB}/\sqrt2 & k_{AB}/\sqrt2 & -k_{BA}-1/T_2\ \pi i(\nu_1^B+\nu_2^B) & \pi i(\nu_2^B-\nu_1^B)\\ -(1-2p)k_{AB}/\sqrt2 & -(1-2p)k_{AB}/\sqrt2 & \pi i(\nu_2^B-\nu_1^B) & -k_{BA}-2k_{BB}-1/T_2+\pi i(\nu_1^B+\nu_2^B+2J)\end{vmatrix}\begin{vmatrix}\rho_{12}^A\\\rho_{13}^A\\\sigma_{12}^B\\\sigma_{13}^B\end{vmatrix} \quad (29)$$

$$\frac{d}{dt}\begin{pmatrix}\rho_{24}^A \\ \rho_{34}^A \\ \sigma_{24}^B \\ \sigma_{34}^B\end{pmatrix}=\begin{pmatrix} -k_{AB}-k_{AA}-\tau V_0 +2\tau i(\nu_2^A-J^A/2) & k_{AA}+\tau i J^A & k_{BA}/\sqrt{2} & (1-2p)k_{BA}/\sqrt{2} \\ k_{AA}+\tau i J^A & -k_{AB}-k_{AA}-\tau V_0+2\tau i(\nu_1^A-J^A/2) & k_{BA}/\sqrt{2} & -(1-2p)k_{BA}/\sqrt{2} \\ k_{AB}/\sqrt{2} & k_{AB}/\sqrt{2} & -k_{BA}-\tau V_0 \; \tau i(\nu_1^{A2}+\nu_2^{A2}) & \tau i(\nu_2^B-\nu_1^B) \\ -(1-2p)k_{AB}/\sqrt{2} & -(1-2p)k_{AB}/\sqrt{2} & \tau i(\nu_2^{A2}-\nu_1^{A2}) & -k_{BA}-2k_{BB}-\tau V_0 +\tau i(\nu_1^B+\nu_2^B-2J)\end{pmatrix}\begin{pmatrix}\rho_{24}^A \\ \rho_{34}^A \\ \sigma_{24}^B \\ \sigma_{34}^B\end{pmatrix} \tag{30}$$

There are two cases where this two—site model reduces to the simpler one—site model discussed in the previous section. In case (i) the population of B is so small that B can be considered as an intermediate for which the well—known steady state approximation applies. In this case the formal kinetic theory of chemical reactions leads to the following expression for the rate of incoherent exchange

$$k = k_{AA} + k_{AB}[k_{BB}+2p(1-p)k_{BA}]/(2k_{BB}+k_{BA}). \tag{31}$$

When $p = 0$ or 1 it follows in the case of a fast interconversion between A and B i.e. if $k_{BA} >> 2k_{BB}$ that

$$k = k_{AA} + K_{AB}k_{BB}, \; K_{AB} = k_{AB}/k_{BA} = x_B/x_A. \tag{32}$$

In the case where $2k_{BB} >> k_{BA}$ we obtain

$$k = k_{AA} + k_{AB}/2. \tag{33}$$

Now, every other interconversion between A and B leads to an incoherent dihydrogen exchange. On the other hand, if $p = 0.5$ in Eq. (30) we obtain exactly the same result of Eq. (32) indicating that k_{BB} is no longer important.

In case (ii) k_{BA} and k_{AB} are larger than the chemical shift differences occuring in A and B, but both species may be present in comparable concentrations. In this case we obtain the average chemical shifts

$$\nu_i = x_A\nu_i^A + x_B\nu_i^B, \; i = 1, 2. \tag{34}$$

In principle, one can define the average coupling constant

$$J = x_A J^A + x_B J^B = (J^A + K_{AB} J^B)/(1 + K_{AB}) \tag{35}$$

which can, however, only by observed when $p = 0$ or 1 and k_{AA} and k_{BB} are small as discussed below.

In the calculated spectra of Fig. 4 the direct mutual exchange rate k_{AA} was set to zero, as well as J^A. In the series of spectra of Fig. 4a also k_{BB} and p were set to zero. K_{AB} was set arbitrarily to a value of 0.9. From the bottom to the top the rate constant k_{AB} was increased. In the slow exchange regime (bottom) three singlets are obtained at ν_1^A and ν_2^A for the A – form and a smaller one $\nu_1^B \approx \nu_2^B$ for the B form. As k_{AB} is increased the lines broaden. They do not coalesce, but give eventually rise to the typical four line two–spin splitting pattern, characterized by the average chemical shifts ν_1 and ν_2, and the average coupling constant J given by Eqs. (34 – 35). If $x_B \ll x_A$ and $J^A \approx 0$ it follows that $\nu_1 \approx \nu_1^A$ and $\nu_2 \approx \nu_2^A$ and that $J \approx x_B J^B = K_{AB} J^B$. Thus, for the observation of the exchange coupling, only the quantity

$$Q = [\frac{x_B J^B}{\nu_1^A - \nu_2^A}]^2 \tag{36}$$

is of importance. This is a lucky situation because a large chemical shift difference for the two coupled hydrogen spins is "borrowed" from the dihydride state A and the large exchange coupling which is not directly observable in the dihydrogen state B is scaled by the factor x_B due to the fast interconversion between the two forms.

It is noteworthy that the fast interconversion between A where $J^A \approx 0$ and B where the frequency of coherent dihydrogen exchange is large, i.e. $J^B \gg |\nu_1^B - \nu_2^B|$ does not lead *a priori* to an incoherent mutual exchange of the two hydrogen nuclei. This incoherent mutual exchange between $\alpha\beta$ and $\beta\alpha$ can, however, be switched on by increasing either the rate constants k_{AA} or k_{BB}, or by setting $p = 0.5$, leading to the effects depicted in Fig. 4b to 4d. No effect is observed in the bottom spectra where the exchange between A and B was suppressed and where the two protons in B can not be distinguished. As can be inferred from Eqs. (29 – 30) the incoherent exchange in B leads to a fast decay with the rate constant $2k_{BB}$ of the forbidden S – T transitions but not of those of the allowed transitions. However, a dramatic effect is observed in the range of the fast interconversion

between B and A, i.e. in the case of the top spectra of Figs. 4a to 4d. As k_{BB} is increased the lines of the signal pattern (Fig. 4a, top) broaden and coalesce into a single line (Fig. 4d, top). This effect corresponds to the apparent transition from the coherent to the incoherent exchange regime, as depicted in Fig. 2b.

The reason of this transition can be inferred by inspection of Eqs. (29 − 30). From these equations it follows that the condition for the observation of an average exchange coupling in the spectra is the formation and the periodic time evolution of the quantum coherences $\sigma_{13}^B = \sigma_{T_1S}^B$ and $\sigma_{34}^B = \sigma_{ST_{-1}}^B$ of the forbidden transitions between the singlet and the triplet states of B. If these coherences are not formed because of $p = 0.5$ or if they decay rapidly because of large values of $2k_{BB}$ the chemical shifts of the two nuclei are averaged and the $J-$ splittings are lost.

In the following we want to study the question whether the two−site−eight−level model can also explain the INS spectra of transition metal dihydrogen complexes? Here tunnel splittings can only be observed if the rotational barriers are very small and the tunnel splittings large. In principle, the rotational tunnel states can be evaluated in the simplest case of a two−fold rotation by solving the one−dimensional Schrödinger equation. Of the manifold of odd and even states we only consider for simplicity the two lowest pairs 0 and 1 of singlet and triplet states, as depicted schematically in Fig. 5. The subscripts used in the following discussion now refer to the numbering of the level pairs. As is well known [6a,10] the lowest splitting $J_0 = E_{T_0} - E_{S_0} > 0$ and the upper one $J_1 = E_{T_1} - E_{S_1} <$ 0. The incoherent 0−1 interconversion can be characterized by the two forward and backward rate constants k_{01} and k_{10}, i.e. in principle by the exchange network of Fig. 3. We obtain the following density matrix equation similar to the well−known asymmetric two−site system

$$\frac{d\sigma_{S_0T_0}}{dt} = [-k_{01} - \frac{1}{T_2} + \pi i |J_0|]\sigma_{S_0T_0} + k_{10}\sigma_{S_1T_1}, \tag{37}$$

$$\frac{d\sigma_{S_1T_1}}{dt} = [-k_{10} - \frac{1}{T_2} - \pi i |J_1|]\sigma_{S_1T_1} + k_{01}\sigma_{S_0T_0}, \tag{38}$$

$$\frac{d\sigma_{T_0S_0}}{dt} = [-k_{01} - \frac{1}{T_2} - \pi i |J_0|]\sigma_{T_0S_0} + k_{10}\sigma_{T_1S_1}, \tag{39}$$

$$\frac{d\sigma_{T_1S_1}}{dt} = [-k_{10} - \frac{1}{T_2} + \pi i |J_1|]\sigma_{T_1S_1} + k_{01}\sigma_{T_0S_0}, \tag{40}$$

There is a complete correspondence between the NMR spectra of Fig. 4 and the INS spectra calculated using Eqs. $(27 - 40)$, depicted in Fig. 5, where arbitrary parameters were employed. In the slow exchange region all transitions S_0-T_0, T_0-S_0, S_1-T_1, and T_1-S_1 appear in the calculated spectrum at J_0, $-J_0$, J_1 and $-J_1$, weighted by the populations x_0 and x_1. When the rotational excitation occurs, transition S_0-T_0 exchanges with S_1-T_1 and T_0-S_0 with T_1-S_1, i.e. with transitions located on the other side of the elastic line at zero enery. The description in terms of NMR line–shape theory is straightforward. As k_{01} is increased at constant populations (Fig. 5a – 5d) the lines broaden, coalesce to two new averaged lines both shifted to the the center, characterizing the average transition S–T and T–S. The average tunnel splitting in Fig. 5d is again given by Eq. (35), written here as

$$J = x_0 J_0 + x_1 J_1. \tag{41}$$

In Figs. 5e to g, fast exchange between S_0-T_0 and S_1-T_1 was assumed, a small value of k_{oo} and a large value of k_{11} of incoherent exchange in the lower and the upper rotational state pairs. Only the population of x_1 was increased, leading to a further decrease of J i.e. shift of both lines towards the elastic line; at the same time, the average line–width of the quasielastic line increases monotonously with

$$k \approx x_0 k_{oo} + x_1 k_{11} \approx k_{oo} + x_1 k_{11} \tag{42}$$

The line–shift occurs essentially because of the sign inversion of the tunnel splitting upon rotational excitation, the line–broadening because of a short incoherent exchange in the excited state. As in the case of NMR, in this regime the one–site model applies again, taking J and k as temperature dependent thermal averages.

2.4. Inclusion of a large number of sites

The extension to a larger number of sites, i.e. configurations or rovibrational levels characterized by different exchange couplings and rate constants of incoherent exchange is straightforward. In the case where the interconversion between the sites is rapid the simple model of section 2.1. applies again. The difference is that now the chemical shifts ν_1 and

ν_2, the exchange coupling constant J and the rate constant k of incoherent exchange represent averages over many states. The simulation of the NMR and the INS spectra then only leads to these average quantities. Information about the nature of the important states can then no longer be obtained in the stage of spectral simulations but only in a later stage by modeling the dependence of the quantities obtained as a function of temperature.

3. Experimental Results

As experimental examples we firstly present in Fig. 6 the temperature dependent superposed experimental and calculated ^{1}H NMR spectra of the dihydride $Cp_2TaH_2P(OMe)_3$, where Cp ≡ cyclohexadienyl and Me≡CH_3, dissolved in CD_2Cl_2, observed recently [7b]. The assignment of the lines is straightforward. The compound consists of a mixture of the cis–form 1 and the trans form 2. Only 1 exhibits exchange couplings, labeled as J^{HH}, giving rise to the splittings between the two signals and between the signals b. Both sites are further split by scalar magnetic couplings to [31]P. Since the sample was partially deuterated also signals from 1–d are present which do not exhibit exchange couplings. As the temperature is increased the average exchange coupling J^{HH} increases, as well as k^{HH} and k^{HD}. There is almost no kinetic HH/HD isotope effect on the incoherent exchange supporting that it does not involve incoherent thermal activated tunneling, in contrast to other double proton transfer reactions [11]. If the additional coupling to ^{31}P is neglected the situation for 1 corresponds to the situation of Fig. 2b.

By contrast, a situation resembling Fig. 1b and Fig. 2c is realized for $Cp_2TaH_2P(CO)_3$ dissolved in CD_2Cl_2 [7b] as illustrated in Fig. 7. Sites a and b in the partially deuterated compound 3–d are not equivalent at low temperatures; the two signals are split into triplets with a scalar coupling constant of $J^{HD} = 27.5$ Hz, indicating the formation of a dihydrogen pair complexed to Ta; the corresponding coupling constant in free HD is approximatively 300 Hz [12]. The increase of temperature leads to an increase of the rate constant k^{HD} describing the incoherent HD exchange, leading to a broadening and coalescence of the a– and the b–triplets. By contrast, the signal of the c–sites in 3 is a sharp singlet at all temperatures and does not show any decoalescence at low temperatures,

indicating a situation as described in Fig. 2c. Since the kinetic HH/HD isotope effects are small the absence of the decoalescence indicates the presence of a very large quantum coupling constant J which is much larger than the chemical shift difference $|\nu_1-\nu_2|$; therefore the value of J can no longer be detected by NMR.

In principle, this can be done by INS for the tungsten dihydrogen complex $W(PCy)_3(CO)_3(\eta-H_2)$ 4 whose INS spectra have been described previously [3g]. Here we simulated the line–shape associated with the two rotational tunnel transitions of 4 in terms of the one–site model of section 2.2., by adapting J and the lorentzian line–width

$$W = 2k/\pi + W_0. \tag{43}$$

W_0 represents the line–width for $k = 0$. Eq. (43) directly follows from Eq. (25). The resulting superposed experimental and calculated spectra are depicted in Fig. 8, where for the sake of clarity plots of the calculated line–shapes of the outer rotational tunnel transitions of 4 without the contribution of the quasielastic center line are included. J is found to be practically independent on temperature, i.e. varies slightly between 0.12 meV (29 GHz or 0.97 cm^{-1}) at 1.5 K and 0.16 meV (38 GHz or 1.3 cm^{-1}) at 189 K. These values are in good agreement with the value of 0.95 cm^{-1} reported previously for 4.9 K. At low temperatures the tunnel transitions are fairly sharp. The experimental line–shapes seem to be gaussian, but for simplicity we used a lorentzian line–shape which does not lead to a large error. The lorentzian line–widths W obtained by simulation are indicated in Fig. 8. They increase with temperature because of the increase of k with temperature, as expected from Eq. (43) until they disappear. In order to calculate k from Eq. (43) knowledge of the exact value of W_0 is needed. If W_0 is temperature independent and $k(1.5K) << W(1.5K) \approx W_0$ we obtain – assuming an Arrhenius law $k = A\exp(-E_a/RT)$ – values of $E_a \approx 700$ $Jmol^{-1}$ (7.3 meV, 60 cm^{-1}) and $A = 10^{11}$ s^{-1} and $k(189K) \approx 5\cdot10^{10}$ s^{-1}. This activation energy is much smaller than the barrier height of about 8.9 $kJmol^{-1}$ (92 meV, 760 cm^{-1}) calculated from the measured tunnel frequency [3g]. On the other hand, at higher temperatures the contribution of W_0 to W is negligibly small. In this case we estimate from the above value of $k(189K)$ using a value of $A = 10^{13}$ s^{-1} typical for intramolecular proton transfers [11] an energy of activation at high temperature of $E_a \approx 8$

kJmol^{-1} which is of the expected order. On the other hand, one could interpret the data also in terms of Eq. (42), predicting at low temperature a temperature independent value of $k = k_{00}$, and at high temperature a value of $k = x_1 k_{11}$, leading to a non–Arrhenius behavior of ln $W \propto$ ln k vs. $1/T$. The non–Arrhenius behavior of W was noted previously for 4 [3g], and also found for other dihydrogen complexes [3d], but the explanation in terms of Eq. (42) is a result of this study. We note that the temperature independent value of k_{00} would correspond in the case of single proton transfers to the rate constant of incoherent tunneling in the vibrational groundstate.

5. Discussion

In the theoretical section a unified view of coherent and incoherent dihydrogen exchange in transition metal hydrides by nuclear magnetic resonance (NMR) and inelastic neutron scattering (INS) was presented. It was shown that both exchange processes do not transform into each other but are always superimposed although each of them may dominate the spectra in different temperature ranges. This superposition is the consequence of the incorporation of the dihydrogen exchange coupling J into the nuclear spin hamiltonian proposed by Zilm and Weitekamp [5] which enables the use of the well known density matrix theory of exchange broadened NMR line–shapes developped by Alexander and Binsch [9] to describe the incoherent process. This theory was used also to describe the line–shapes of the rotational tunneling transitions observed in the INS spectra of transition metal dihydrogen complexes. Both NMR and INS spectra depend on the same parameters characterizing the coherent and incoherent exchange processes. In particular, two simple models of dihydrogen exchange effects on the NMR and INS spectra were discussed. In the first model a single site two spin system was considered involving four nuclear spin levels, characterized by a single average tunnel freuquency J and a single rate constant k of incoherent dihydrogen exchange. Whereas J leads to the usual NMR line–splitting the increase of k induces line–broadening and coalescence into a single line by averaging of the chemical shifts of the two hydrogen atoms. By contrast, the quantum coherences between the nuclear singlet and triplet states which are not observable by NMR but are seen in INS

as rotational tunneling transitions were predicted to decay with $2k$ leading to a homogeneous broadening of $2k/\pi$ of the corresponding INS bands. This result explains the disappearance of these bands when temperature is raised as k increases monotonously with the latter. Since in practice many sites have to be taken into account, corresponding to different molecular configurations, conformations, solvent environments, or simply different rovibrational states the simple one–site model is only valid in the case of rapid site interconversion where J and k now represent averages over all sites. The process of site interconversion with and without a combined dihydrogen permutation on the NMR an INS spectra was studied in a two–site model, adapted to typical experimental situations encountered in NMR and INS using the Alexander–Binsch theory. One important result of this discussion was that it is not the short lifetimes of a rovibrational nuclear singlet–triplet pair which limits the contribution of this pair to the average J. The determining factor is whether during this lifetime the quantum coherence between the two states is either lost by a fast incoherent exchange according to Fig. 3a or because this coherence is not created at all when the site interconversion is associated to a dihydrogen permutation as illustrated in Fig. 3b. In the experimental section it was shown that the experimental findings can indeed be interpreted using the simple one–site exchange model because the rapid site exchange regime is realized not only in NMR but apparently also in INS of transition metal dihydrogen complexes. The difference between the two methods is only the timescale of J and k; whereas INS is sensitive to the meV i.e. GHz range, NMR is sensitive to the kHz range. However, in both methods there may be other line–broadening mechanisms which have to be discussed. Whereas these are well known in liquid state NMR, it is more difficult in the INS case to estimate linewidth contributions which do not arise from the incoherent dihydrogen exchange. In the case of the INS spectra of the dihydrogen complex 4 (Fig. 8) a relatively small energy of activation and a small frequency factor was observed, as usually typical for incoherent tunneling processes.

In view of the now combined NMR and INS results we will discuss in the remainder of this section some consequences concerning various models of dihydrogen exchange in transition metal hydrides. Finally, we will give a qualitative explanation of the apparent

puzzle of a coexistence of the coherent and the incoherent exchange.

There are several models of coherent dihydrogen exchange in the literature, whose detailed discussion is beyond the scope of this paper. We only state that all models assume a fast interconversion between all rovibrational states and nuclear configurations, leading to averaged values of the exchange couplings J. All models propose more or less a rotation of dihydrogen pairs around an axis between the metal and the dihydrogen center, because in a direct translational exchange both protons would have to go through each other which is impossible. Therefore, the Landesmann model proposed by Zilm et al. [5] implies first a thermally assisted small angle rotation and then translational tunneling of the two protons involving a distance λ of minimal approach. This model predicts an increase of the averaged J with increasing temperature. On the other hand, the rigid rotor model consisting of 180^0 dihydrogen rotations at a fixed dihydrogen distance has been used in order to interpret the INS spectra of transition metal dihydrogen complexes [3]. This model is depicted schematically in Fig. 9a and b. The rotational states are obtained by solution of the Mathieu equation [3,6a,10]. As discussed in the previous section, the symmetry of the wave functions leads to the well—known alternance of the tunnel splittings of the rigid rotor [6a]: the splitting J_0 in the ground state is positive, because the symmetric state of symmetry A (not to be confounded with the different configurations A and B of Fig. 3) linked to the nuclear singlet state has a lower energy and the antisymmetric state of symmetry B linked to the nuclear triplet state a higher one. However, the splitting J_1 in the first excited state is negative because now the A state exhibits the higher energy. Therefore, when the first excited state is populated J decreases. It is easily shown [5a] that excitation of higher rotational levels should lead eventually to $J = 0$ at high temperature as illustrated in Fig. 9d. A more sophisticated non—rigid rotor model exhibits similar features at low temperature, although there is no strong alternance of positive and negative rotational tunneling pairs any more [6e]. The calculations presented in [6e] which predict an increase of J at higher temperatures need, however, to be further corroborated, because the sign of J depends in this regime strongly on the number of rotational level pairs above the barrier included in the calculation, leading to a problem of convergence of the $J -$

values. Experimentally, a decrease of J with increasing temperature has been frequently observed both by INS and NMR in the related case of methyl group rotational tunneling [1,2]. In the case of compound 4 (Fig.8) J does not significantly change with temperature, indicating that within the rigid rotor model the high temperature regime is not reached. However, in the case of other dihydrogen rotations studied by INS clear shifts of J to smaller energies have been observed [3,13] which can be interpreted in terms of the simple model of Fig. 5. In the case of the tantal dihydrogen compound [7] shown in Fig. 7 containing also a side—on dihydrogen one would then expect that J decreases with temperature; unfortunately, the exchange coupling whose existence was proved was so strong that the value of J was much larger than the chemical shift difference of the two protons involved, precluding a direct measurement of J by NMR. On the other hand, the observations by NMR of exchange couplings J in transition metal dihydrides and trihydrides which increase with increasing temperature [4,5] e.g. the tantal dihydride [7] of Fig. 6 is not consistent with a simple rigid or non—rigid rotor tunneling model.

A model which can explain both a decrease or an increase of J with temperature was proposed by some of us [6a] and consists of a series of different configurations illustrated in Fig. 9. In the dihydrogen configuration of Fig. 9a the rotation barrier is large but reduced in the side—on bound dihydrogen complex of Fig. 9b, and vanishes in the case of free dissolved dihydrogen (Fig. 9c). If each configuration J decreases with increasing temperature when the "vertical" rotational excitation occurs at elevated temperatures; however, when starting in the dihydride configuration of Fig. 9a characterized by a large barrier and a very small tunnel frequency a "lateral" thermal excitation will lead to the dihydrogen configuration of Fig. 9b leading first to an increase of J because of the large J_0 in this site; only later the decrease is expected according to the calculation of Fig. 9e. Thus, when lateral excitation dominates over the vertical excitation J will further increase as indicated in Fig. 9f until free dihydrogen is formed.

Unfortunately, the J values of transition metal dihydrides are too small to be studied by INS, and the experimental temperature range where J can be evaluated by NMR is limited by the on—set of incoherent exchange at high temperatures characterized

by the average rate constant k, which also leads to INS line—broadening and disappearence (Fig. 5). In NMR it leads to an averaging of the chemical shifts and, therefore, to a disappearence of J from the spectra as depicted in Figs. 2 and 4, although the average J still exists in principle. The incoherent exchange in the case of the tantal dihydride of Fig. 6 was found to exhibit a surprisingly small kinetic HH/HD isotope effect, i.e. it cannot arise from an incoherent tunnel process which should imply much larger effects [11]. Therefore, it must correspond to a over—barrier rotation either in a dihydride configuration (Fig. 9a), a dihydrogen configuration (Fig. 9b) or in a configuration involving loosely bound or almost free dihydrogen. The absence of any kinetic isotope effect on the incoherent exchange could arise from a ligand reorientation in the rate limiting reaction step. A complete dihydrogen dissociation—recombination mechanism can be excluded in most cases where the scalar coupling of dihydrogen to other nuclei such as ^{31}P is not destroyed by this process. It is, however, important to note that the configurations determining the rate constants k of the incoherent exchange are not necessarily the same as those determining the exchange couplings J.

This incoherent exchange is superimposed to the coherent exchange, as discussed above. This conclusion was reached as follows. As depicted in Fig. 1, the magnetic field breaks the symmetry of the spins if they experience different chemical shifts. Then, only the spin states $\alpha\alpha$ and $\beta\beta$ are delocalized coherent tunnel states but not $\alpha\beta$ and $\beta\alpha$ which are states localized by the magnetic field. The incoherent exchange from $\alpha\beta$ to $\beta\alpha$ has the property, in contrast to the coherent exchange, to lead to a permutation of the chemical shifts of the two nuclei, in a similar way as a permutation of the pair H—D to D—H. Therefore, the incoherent process leads to line—broadening and line—coalescence of the two hydrogen signals, in contrast to the exchange coupling. A puzzling question then arises concerning the nature of the incoherent exchange of dihydrogen in the absence of a magnetic field, where the two nuclei are no longer labeled by their spins, in contrast to the HD and the DH groups in a molecule. It was shown in the theoretical section that the incoherent process is still defined for a coherently exchanging or rotating H_2 pair even outside a magnetic field: here, $2k$ represents the decay time constant of the quantum

coherence between the nuclear singlet and triplet states which normally oscillates with the tunnel frequency. This decay is the key quantity in the transition from the coherent to the incoherent tunneling regime because a thermally populated state pair r normally contributing the value $x_r J_r$ to the average exchange coupling will also contribute the value $2x_r k_{rr}$ to the average rate constant k of incoherent exchange. Therefore, the criterium of whether a singlet–triplet state pair contributes to J or not is not given by its lifetime τ_r but by the condition $2k_{rr} << 1/\tau_r$. In other words, the singlet–triplet quantum coherence in the state r must evolve periodically with the frequency J_r and must not decay during its lifetime, otherwise the formation of this state is equivalent to a permutation of the two spins with the probability $p = 0.5$, leading to an averaging of their chemical shifts and to a disappearence of the term $x_r J_r$ in J.

What determines then the rate constant k_{rr}? On one hand it is the rate constant of incoherent dihydrogen exchange, and on the other hand half the decay constant of the loss of singlet–triplet quantum coherence in r. The following qualitative discussion gives a tentative explanation of the fact that both processes are identical and superimposed on the coherent exchange. According to the time–dependent Schrödinger equation spatial wave functions evolve periodically with a frequency given by their energy, as illustrated in Fig. 10 for free or bound H_2 in the nuclear singlet (p–H_2) and the nuclear triplet state (o–H_2). When a sudden 180⁰ jump occurs the spatial wave function of the triplet state changes its sign, in contrast to the wave function of the singlet state. One can then imagine that for an ensemble of o–H_2 molecules with coherently superposed wave functions at $t = 0$ the latter rapidly become out of phase. In the case of bound dihydrogen this is equivalent to the statement that the quantum coherence between the S– and T– states disappears with the rate constant $2k$ of the incoherent 180⁰ rotation. For free o–H_2 dissolved in liquids such sudden changes are well established, and can be described with a rotational correlation time, leading to the spin–rotation relaxation mechanism [14]. In other words, although H_2 is a quantum rotor, the axis characterizing the nodal plane of o–H_2 is subject to rotational diffusion in a similar way as the HD molecule [14]. A similar phenomenon should exist for states of bound dihydrogen situated above the barrier of rotation. One could speculate that

for states situated below the barrier sudden incoherent 180^0 jumps could be possible via incoherent tunneling processes. The latter do not affect the spatial wave functions in the case of a spatially symmetric nuclear singlet states but they alter suddenly the sign of the spatial wave function in the case of the spatially antisymmetric nuclear triplet states. The assumption of such incoherent rotational tunneling process superimposed to the coherent process would open up the possibility to calculate the rate constants of incoherent tunnel processes using dynamic theories. Anyway, further theoretical work is needed in order to justify the concept of superposed coherent and incoherent rotational dihydrogen tunneling. At present, it is tempting to use this concept in order to explain the non–Arrhenius behavior of the incoherent dihydrogen exchange established for the dihydrogen complex 4, assuming that the contributions of other processes to the INS–lineshapes are negligible and that the rovibrational relaxation is fast in the INS timescale. On the other hand, incoherent tunneling is not compatible with the absence of kinetic HH/HD isotope effects found for the incoherent dihydrogen rotation in 1 (Fig.6); as mentioned above, one could invoke a ligand reorientation in the rate limiting step in order to explain these findings. Since it is plausible that such ligand motions could be slower in the solid as compared to the liquid state, or even suppressed, the study of liquid–solid state effects on the incoherent and coherent dihydrogen exchange in transition metal complexes is a challenging task for the future.

4. Conclusions

It has been shown that the inclusion of the quantum exchange into the nuclear spin hamiltonian allows to use the phenomenological NMR line–shape theory of chemical exchange developed by Alexander and Binsch in order not only to calculate NMR but also INS spectra, thus, connecting these two methods and providing a better understanding of many so far unexplained experimental observations. In particular, the possibility of superposed incoherent and coherent dihydrogen tunneling in transition metal hydrides has been addressed theoretically, and supported to some extent experimentally. The approach described here could also be extended in a relatively simple way to the problem of other

group rotations, e.g. methyl group and ammonium group rotational tunneling. Naturally, the simple models developped may be further expanded and refined. Currently, some of us [15] are studying with the methods described in this paper the pathways of spin–polarized dihydrogen incorporation into transition metal complexes [16] as intermediates of the hydrogenation of unsaturated hydrocarbons. Thus, we hope to contribute to a general understanding of the structure and the reactivity of transition metal hydrides.

Acknowledgements

Appendix

The usual nuclear spin functions of a pair of two protons H_a and H_b located in two molecular sites 1 and 2

$$\Psi_1 = \alpha\alpha, \tag{A1}$$

$$\Psi_2 = c_{22}\alpha\beta + c_{23}\beta\alpha, \tag{A2}$$

$$\Psi_3 = c_{32}\alpha\beta + c_{33}\beta\alpha, \tag{A3}$$

$$\Psi_4 = \beta\beta, \tag{A4}$$

can easily be converted into functions satisfying the Pauli Exclusion principle using the identies

$$\alpha\alpha \equiv \tfrac{1}{\sqrt{2}}[\psi_1(a)\psi_2(b)-\psi_2(a)\psi_1(b)]\alpha(a)\alpha(b), \tag{A5}$$

$$\alpha\beta \equiv \tfrac{1}{\sqrt{2}}[\psi_1(a)\psi_2(b)\alpha(a)\beta(b)-\psi_2(a)\psi_1(b)\beta(a)\alpha(b)], \tag{A6}$$

$$\beta\alpha \equiv \tfrac{1}{\sqrt{2}}[\psi_1(a)\psi_2(b)\beta(a)\alpha(b)-\psi_2(a)\psi_1(b)\alpha(a)\beta(b)], \tag{A7}$$

$$\beta\beta \equiv \tfrac{1}{\sqrt{2}}[\psi_1(a)\psi_2(b)-\psi_2(a)\psi_1(b)]\beta(a)\beta(b), \tag{A8}$$

where the product $\psi_1(a)\psi_2(b)\alpha(a)\beta(b)$ represents the configuration where H_a in spin state α is located in site 1 and H_b in spin state β in site 2. Thus, $\alpha\beta$ means that a spin α is located in site 1 and β in site 2, either H_a of H_b.

References

[1]   a: D. Smith, Chem.Rev. *94*, 1567 (1994); b: S. Clough, *Physica B202*, 256 (1994) and references cited therein.

[2]   a: T. K. Jahnke, W. Müller–Warmuth, M. Bennati, Solid State NMR *4*, 153 (1995) and references cited therein; b: A. Heuer, Z.Phys. *B88*, 39 (1992).

[3]   a:G. J. Kubas, R. R. Ryan, B. I. Swanson, P. J. Vergamini, H. J. Wasserman, J. Am.Chem.Soc. *116*, 451 (1984); b: G. J. Kubas, Acc.Chem.Res. *21*, 120 (1988); c: G. Rattan, G. J. Kubas, C. J. Unkefer, L. S. Van Der Sluys, K. A. Kubat–Martin, J. Am.Chem.Soc. *112*, 3855 (1990); d: L. S. Van Der Sluys, J.Eckert, O. Eisenstein, J. H. Hall, J. C. Huffman, S. A. Jackson, T. F. Koetzle, G. J. Kubas, P. J. Vergamini, K. G. Caulton, J.Am.Chem.Soc., *112*, 4831 (1990); e: J. Eckert, G. J. Kubas, J.Phys.Chem. *97*, 2378 (1993); f: J. Eckert, G. J. Kubas, R.. P. White, Inorg.Chem. *31*, 1550 (1993); g: J.Eckert, G.J.Kubas, A.J.Dianoux, J.Chem.Phys., 466 (1988); h: J. Eckert, C. M. Jensen, G. Jones, E. Clot, O. Eisenstein, J.Am.Chem.Soc., *115*, 11056 (1993).

[4]   a: T. Arliguie, B. Chaudret, J. Devillers, R. Poilblanc, C.R.Acad.Sci. Paris, Série II, *305*, 1523 (1987); b: A. Antinolo, B. Chaudret, G. Commenges, M. Fajardo, F. Jalon, R. H. Morris, A. Otero, C. T. Schweitzer, J.Chem.Soc.Chem.Comm. 1210 (1988); d: T. Arliguie, C. Border, B. Chaudret, J. Devilles, R. Poilblanc, Organo-metallics, *8*, 1308 (1989); e: T. Arliguie, B. Chaudret, F. A. Jalon, A. Otero, J. A. Lopez, F. J. Lahoz, Organometallics *10*, 1888 (1991); f: R. R. Paciello, J. M. Manri-quez, J. E. Bercaw, Organometallics, *9*, 260 (1990); g: D. M. Heinekey, N. G. Payne, G. K. Schulte, J.Am.Chem.Soc. *110*, 2303 (1988); g: D. M. Heinekey, J. M. Millar, T. F. Koetzle, N. G. Payne, K. W. Zilm, J.Am.Chem.Soc. *112*, 909 (1990); h: H. H. Limbach, G. Scherer, L. Meschede, F. Aguilar–Parrilla, B. Wehrle, J. Braun, Ch. Hoelger, H. Benedict, G. Buntkowsky, W. P. Fehlhammer, J. Elguero, J. A. S. Smith, B. Chaudret, NMR Studies of Elementary Steps of Hydrogen Transfer in Condensed Phases.in Ultrafast Reaction Dynamics and Solvent Effects, Experimental and Theoretical Aspects, Chapter 2, Eds. Y. Gauduel and P. J.

Rossky, American Institute of Physics, 1994, p. 225.

[5] a: K. W. Zilm, D. M. Heinekey, J. M. Millar, N. G. Payne, P. Demou, J.Am.Chem. Soc. *111*, 3088 (1989); b: K. W. Zilm, D. M. Heinekey, J. M. Millar, N. G. Payne, S. P. Neshyba, J. C. Duchamp, J. Szczyrba, J.Am.Chem.Soc. *112*, 920 (1990); c) K. W. Zilm, J. M. Millar, Adv.Magn.Reson. *15*, 163 (1990); d: S. J. Inati, K. W. Zilm, Phys.Rev.Lett. *68*, 3273 (1992); f: D. Jones, J. A. Labinger, J. Weitekamp, J.Am.Chem.Soc. *111*, 3087 (1989); e: S.Szymanski, J.Mol.Struct. *321*, 115 (1994).

[6] a: H. H. Limbach, G. Scherer, M. Maurer, B. Chaudret, Ang.Chem. *104*, 1414 (1992); Ang.Chem.Int.Ed.Engl. *31*, 1369 (1990); b: J. C. Barthelat, B. Chaudret, J. P. Dauday, Ph. De Loth, R. Poilblanc, J.Am.Chem.Soc. 1991, *113*, 9896 c: A. Jarid, M. Moreno, A. Lledós, J. M. Lluch, J. Bertrán, J.Am.Chem.Soc., *115*, 5861 (1993); d: A. Jarid, M. Moreno, A. Lledós, J. M. Lluch, J. Bertrán, J.Am.Chem.Soc. *117*, 1069 (1995); e: E. Clot, C. Leforestier, O. Eisenstein, M. Pélissier, J.Am.Chem.Soc. *117*, 1797 (1995); f: E. M. Hiller, R. A. Harris, J.Chem.Phys. *98*, 2077 (1993); f: ibid., *99*, 7652 (1993); g: ibid., *100*, 2522 (1993).

[7] a: B. Chaudret, H. H. Limbach, C. Moise, C.R.Acad.Sci. Paris, Série II, *315*, 533 (1992) b: S.Sabo–Etienne, B.Chaudret, H.A.El–Makarim, J.C.Barthelat, J.P.Daudey, S.Ulrich, H.H.Limbach, C.Moïse, J.Am.Chem.Soc., in press.

[8] a: J. W. Emsley, J. Feeney, L. H. Sutcliffe, High Resolution Nuclear Magnetic Resonance Spectroscopy, Vol. 1, Pergamon Press, Oxfdord 1965; b: A. Abragam, The Principles of Nuclear Magnetism, Clarendon Press, Oxford 1961; c: R. R. Ernst, G. Bodenhausen, A. Wokaun, Principles of NMR in One and Two Dimensions, Clarendon Press, Oxford 1987.

[9] a: S.Alexander, J.Chem.Phys. *37*, 971 (1962); b: G. Binsch, J.Am.Chem.Soc., *91*, 1304 (1969); c: D. A: Kleier, G. Binsch, J. Magn. Reson., *3*, 146 (1970).

[10] D. Wallach, W. A. Steele, J.Chem.Phys. 1976,52, 2534; b: National Bureau of Standards, Tables relating to Mathieu functions, Columbia Univ. Press New York, New York 1951.

[11] H. H. Limbach, Dynamic NMR Spectroscopy in the Presence of Kinetic Hydrogen

Deuterium Isotope Effects", Chapter 2, in "NMR Basic Principles and Progress",
Vol. *26*, Berlin Heidelberg New York 1990.

[12] P. E. Bloyce, A. J. Rest, I. Whitwell, W. A. G. Graham, A. J. H. Holmes–Smith,
J.Chem.Soc.Chem.Comm. 846 (1988).

[13] J. Eckert, unpublished results.

[14] a: I. F. Silvera, Rev. Mod. Phys. *52*, 393 (1980); b: A. Abragam, The Principles of
Nuclear Magnetism, Clarendon Press, Oxford 1961.

[15] G. Buntkowsky, J. Bargon, H. H. Limbach, in preparation.

[16] a: C. R. Bowers, D. P. Weitekamp, Phys.Rev.Lett. *57*, 2645 (1986); b: M. G.
Pravic, D. P. Weitekamp, Chem.Phys.Lett. *145*, 255 (1988); c: C. R. Bowers, D. P.
Weitekamp, J.Am.Chem.Soc. *109*, 554 (1987); d: C. R. Bowers, D. H. Jones, N. D.
Kurur, J. A. Labinger, M. G. Pravica, D. P. Weitekamp, Adv.Magn.Reson. *15*, 269
(1990); e: R. U. Kirss, T. Eisenschmidt, R. Eisenberg, J.Am.Chem.Soc., *110*, 8564
(1988); f: R. Eisenberg, Acc.Chem.Res. 1991, 24, 110; g: J. Bargon, J. Kandels, P.
Kating, J.Chem.Phys. *98*, 6150 (1993); h: J. Bargon, J. Kandels, P. Kating, A.
Thomas, K. Woelk, Tetrahedron Letters, *31*, 5721 (1990); i: J. Bargon, J. Kandels,
K. Woelk, Ang.Chem. *102*, 70 (1990); Ang.Chem.Int.Ed.Engl. 29, 58 (1990).

Figure Captions

Fig. 1

Energy level diagram of a pair of hydrogen atoms exhibiting a barrier of exchange. a and b: the magnetic field B >> 0; c: B = 0. ν_1 and ν_2 are the Larmor frequencies or chemical shifts, $J = J_{exch} + J_{magn}$ the sum of the exchange coupling i.e. the coherent tunnel frequency describing the exchange and the scalar magnetic coupling.

Fig. 2

a–c: Calculated ^{1}H NMR spectra of a transition metal dihydride as a function of the coupling constant J arising dominantly from the coherent dihydrogen exchange and of the rate constant k of the incoherent dihydrogen exchange. d: Dependence of the line–shape of the tunnel transition between the nuclear singlet and triplet states as a function of k at B=0 calculated by the usual NMR line–shape theory represented by Eqs. (1 − 3). This transition is forbidden in NMR but allowed in INS; the calculated broadening is presented as the main origin of the disappearence of the INS transitions at high temperature.

Fig. 3

Reaction network of interconversion between two sites A and B each containing a proton pair leading to four nuclear spin states. $p = 0$ or 1 in the absence and $p = 0.5$ in the presence of dihydrogen scrambling during the interconversion. A and B may represent two different rovibrational states, configurations e.g. dihydride and dihydrogen, conformations, solvent environments etc.

Fig. 4

Calculated ^{1}H NMR spectra in the presence of the reaction network of Fig. 3 using arbitrary parameters. The molefractions x_A and x_B were kept constants.

Fig. 5

Calculated INS spectra of a hypothetical transition metal dihydrogen complex in the presence of exchange between the rotational states 0 and 1. a to d: k_{10} was increased at constant values for x_0 and x_1; e to g: $k_{10} >> |J_1 - J_0|$, $k_{11} >> 0$, and only x_2/x_1 was increased from d to f.

Fig. 6

Superposed experimental and calculated 250 MHz ^{1}H NMR signals of the hydride region of a mixture of **1**, **1–d**, **2**, **2–d** dissolved in dioxane–d_8, adapted from Ref. 7b. The signal spacing between the peaks labeled as a indicates the exchange coupling constant J^{HH}.

Fig. 7

Superposed experimental and calculated 250 MHz ^{1}H NMR signals of the hydride region of a mixture of **3** and **3–d** dissolved in CD_2Cl_2, adapted from Reference 7b.

Fig. 8

Superposed experimental and calculated INS spectra of $W(PCy)_3(CO)_3(\eta-H_2)$ as function of temperature. Some of the spectra were previously reported in Ref. [3g]. W is the total linewidth according to Eq. (42); J is the rotational tunnel splitting. For further explanation see text.

Fig. 9

One–dimensional slices along the reaction pathway of dihydrogen exchange. a and b: situations typical for dihydride and dihydogen configurations, c: free dissolved dihydrogen. d to e: expected dependences of the average exchange coupling on temperature. For further explanation see text.

Fig. 10

The effect of sudden 180° jumps on the time dependence of the spatial wave function of bound and/or free p–H_2 and o–H_2.
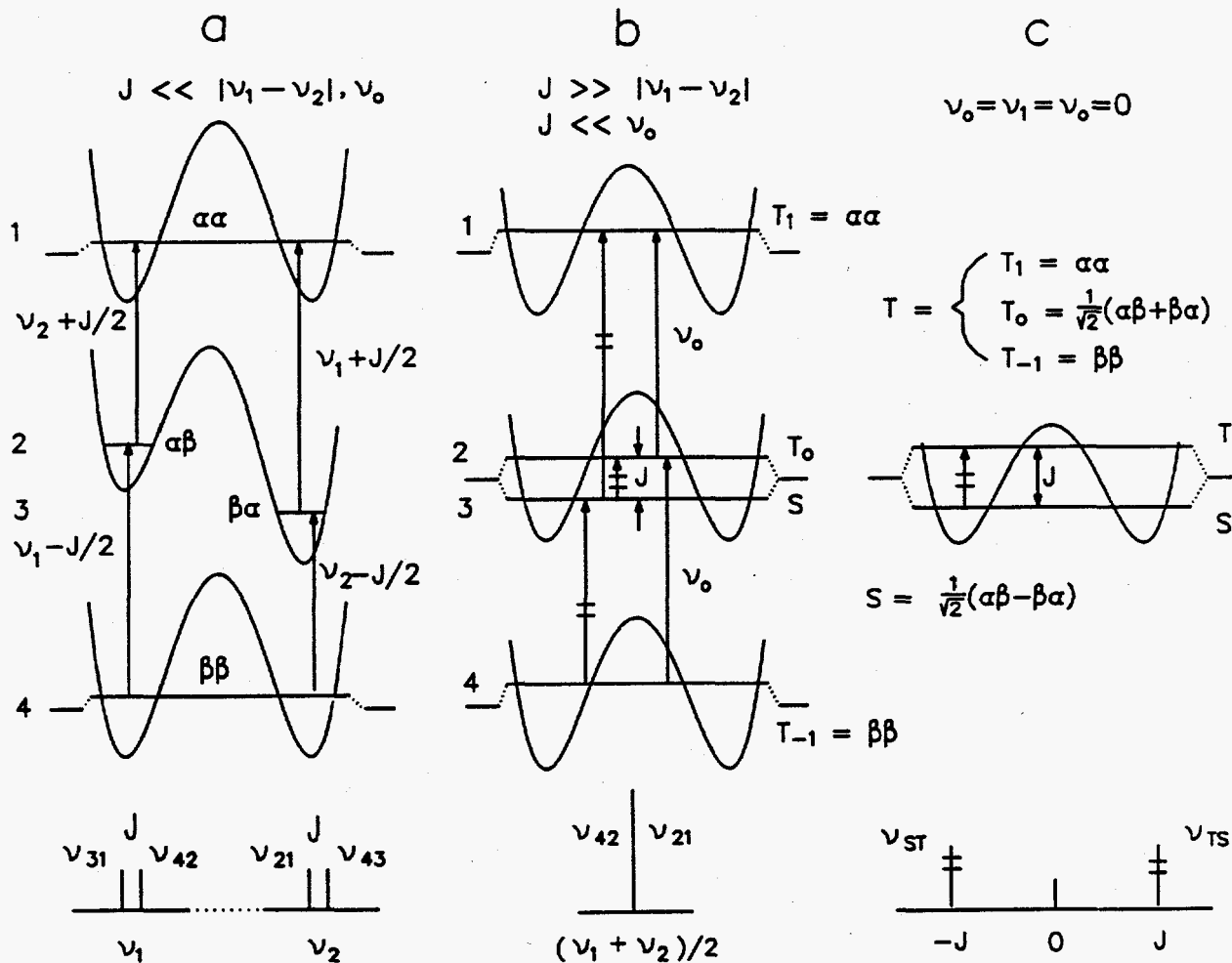
Figure 1 Limbach et al.
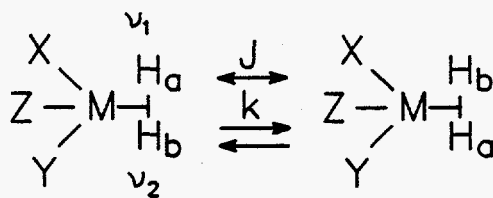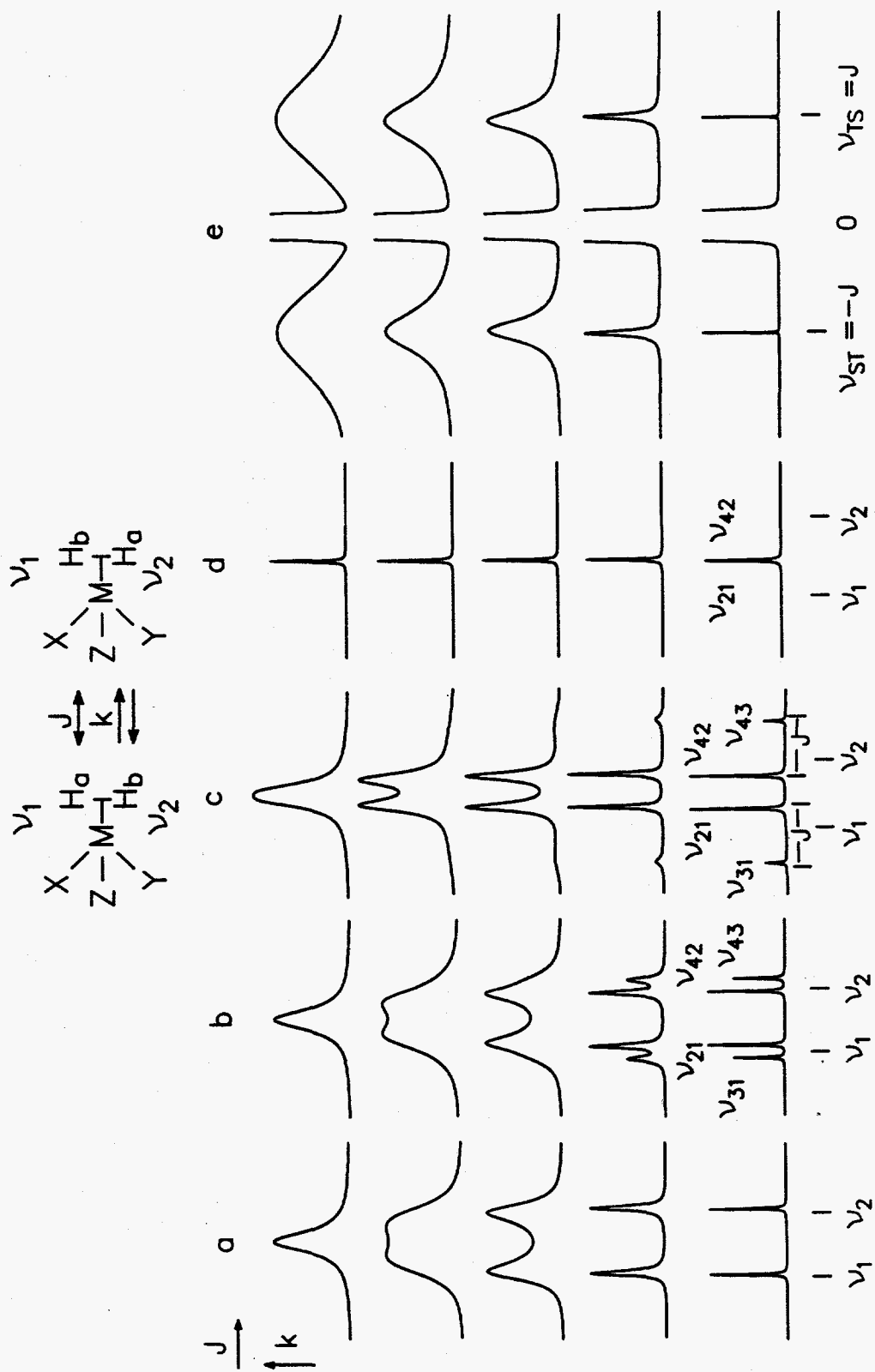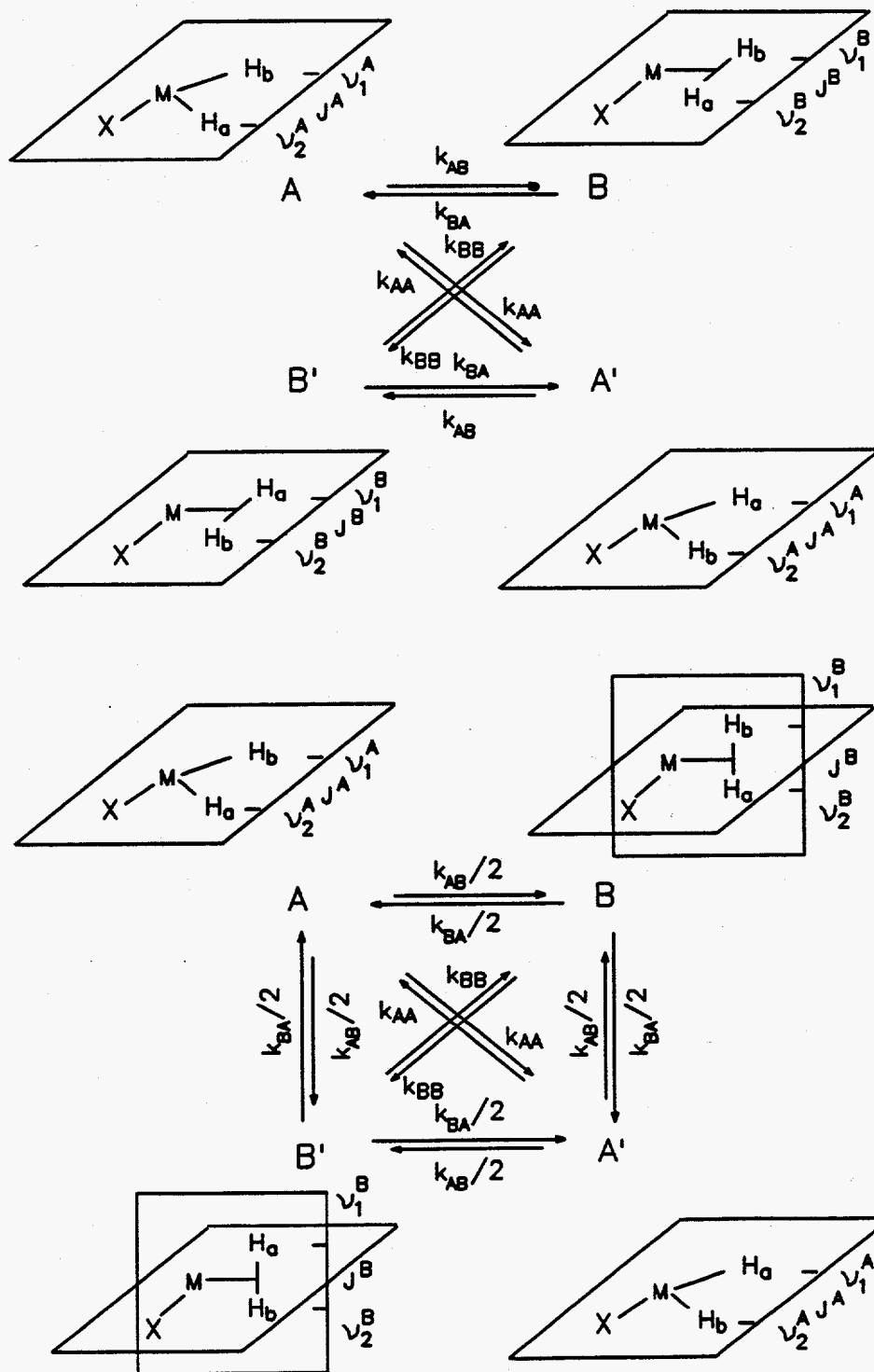
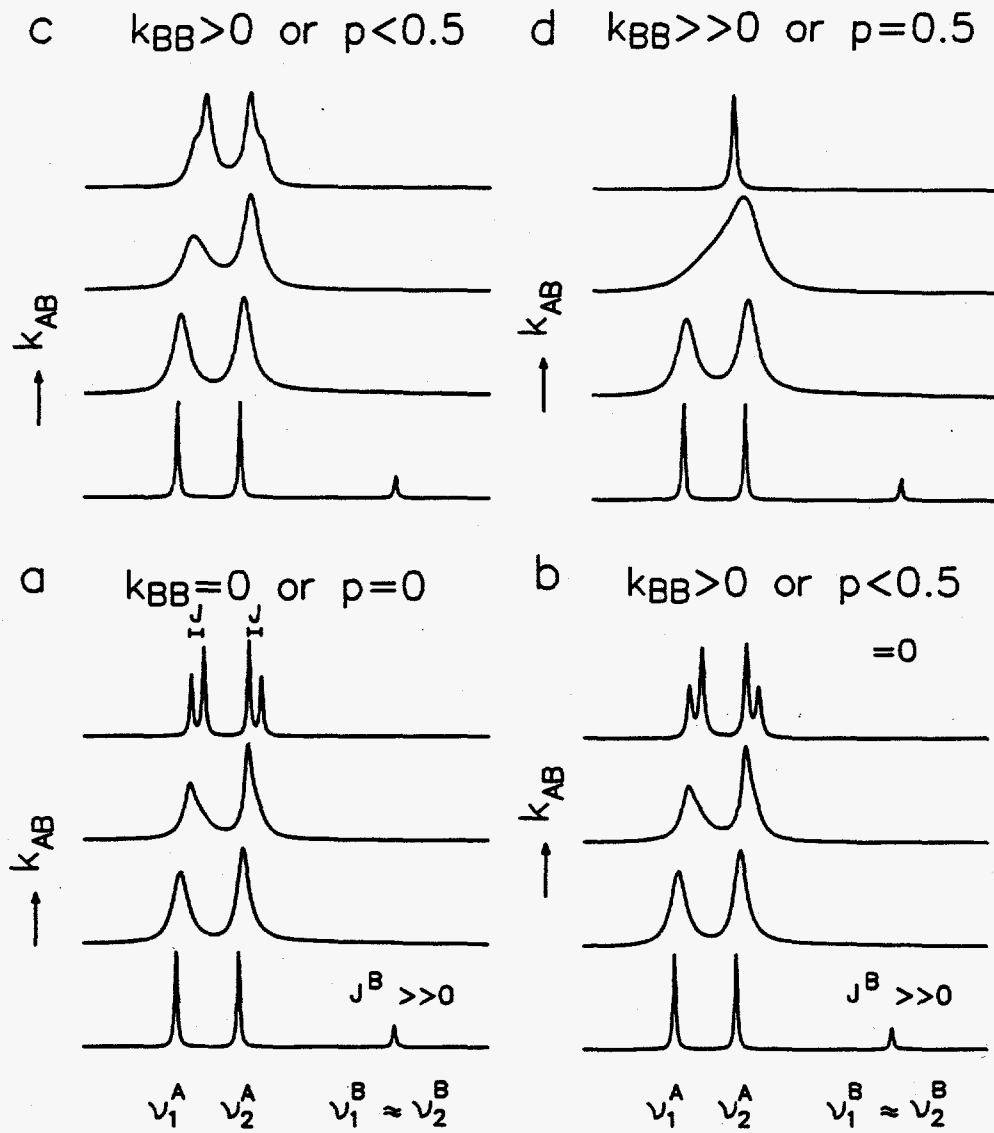Figure 2 Limbach et al.

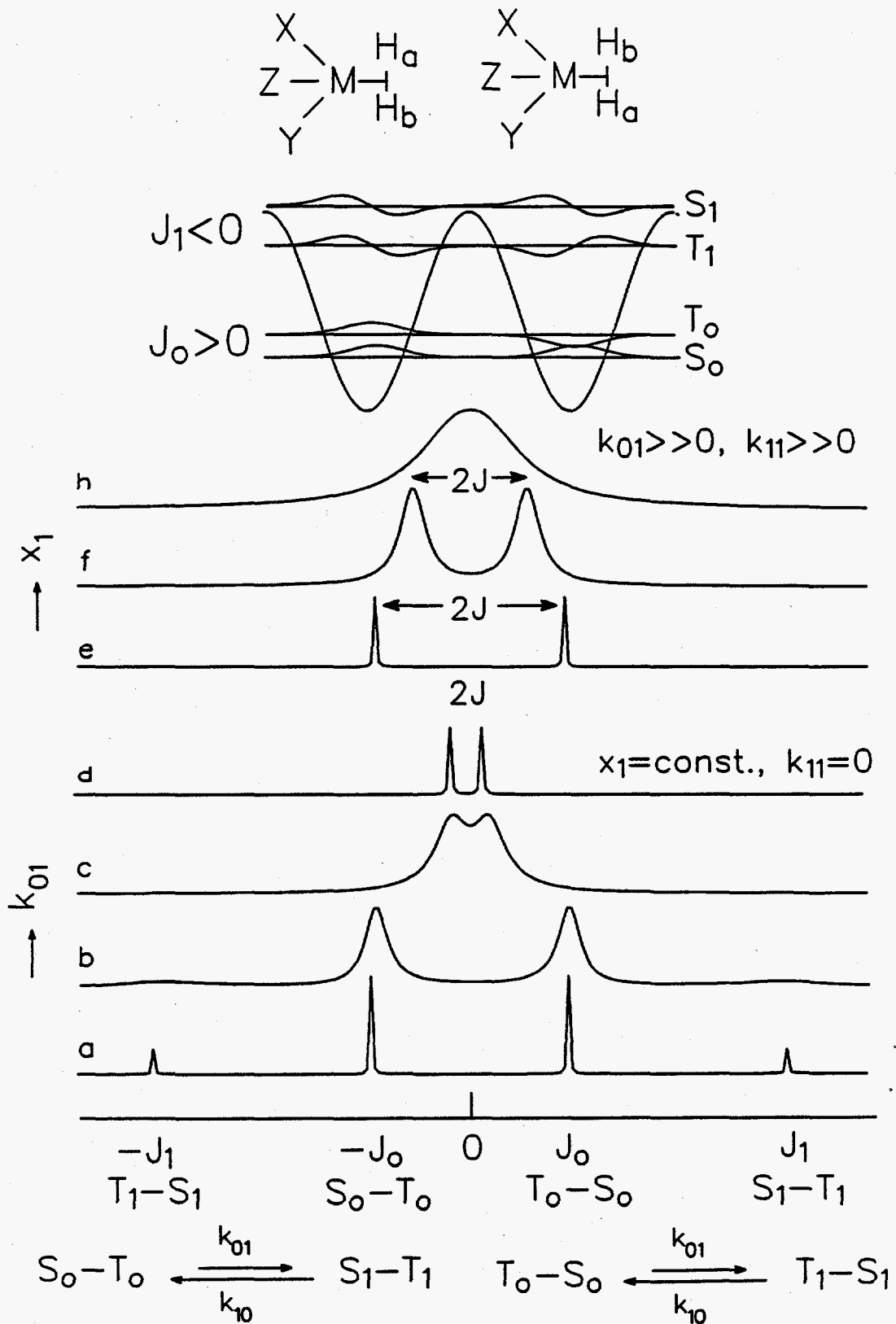Figure 3 Limbach et al.

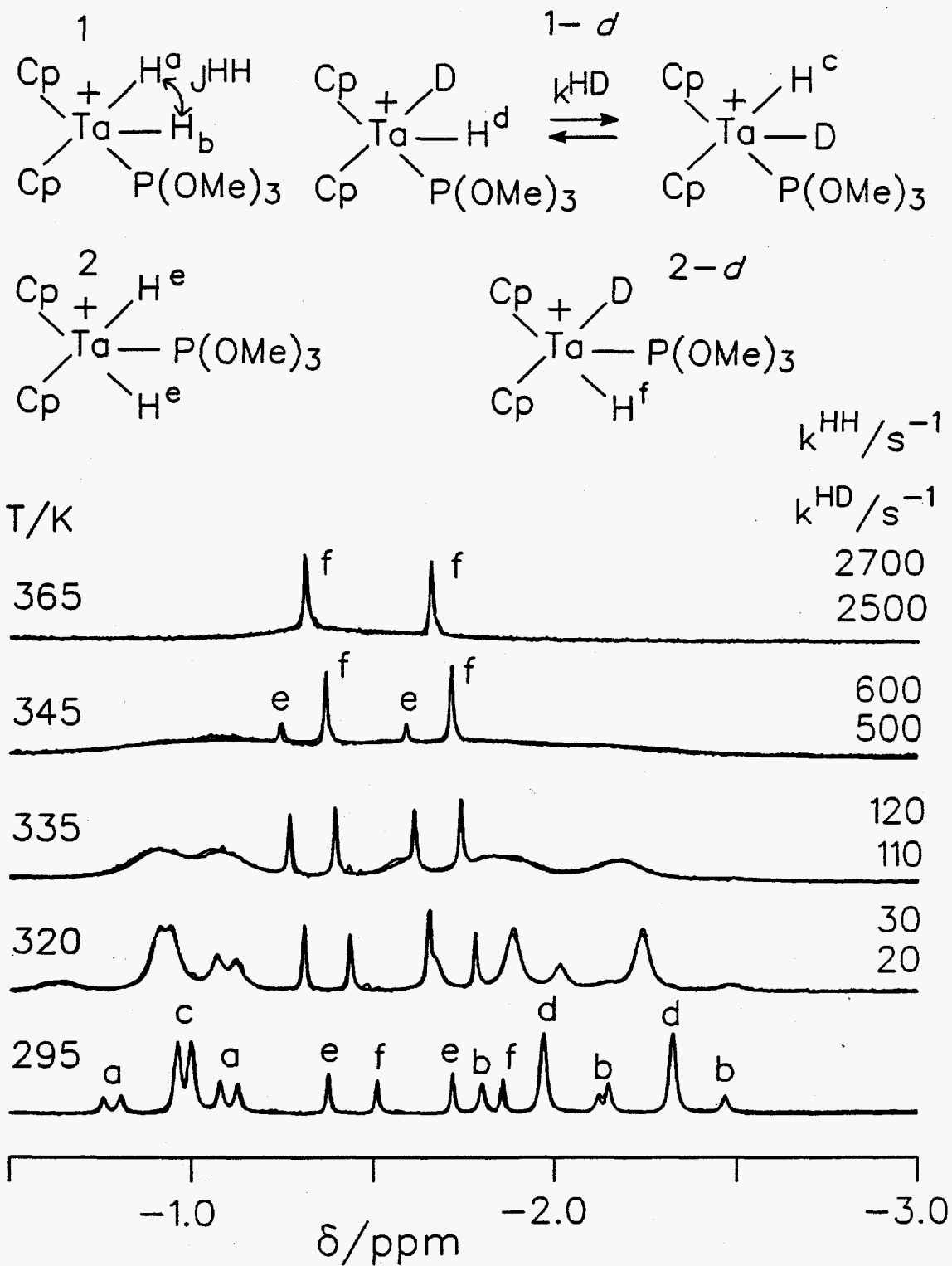Figure 4 Limbach et al.

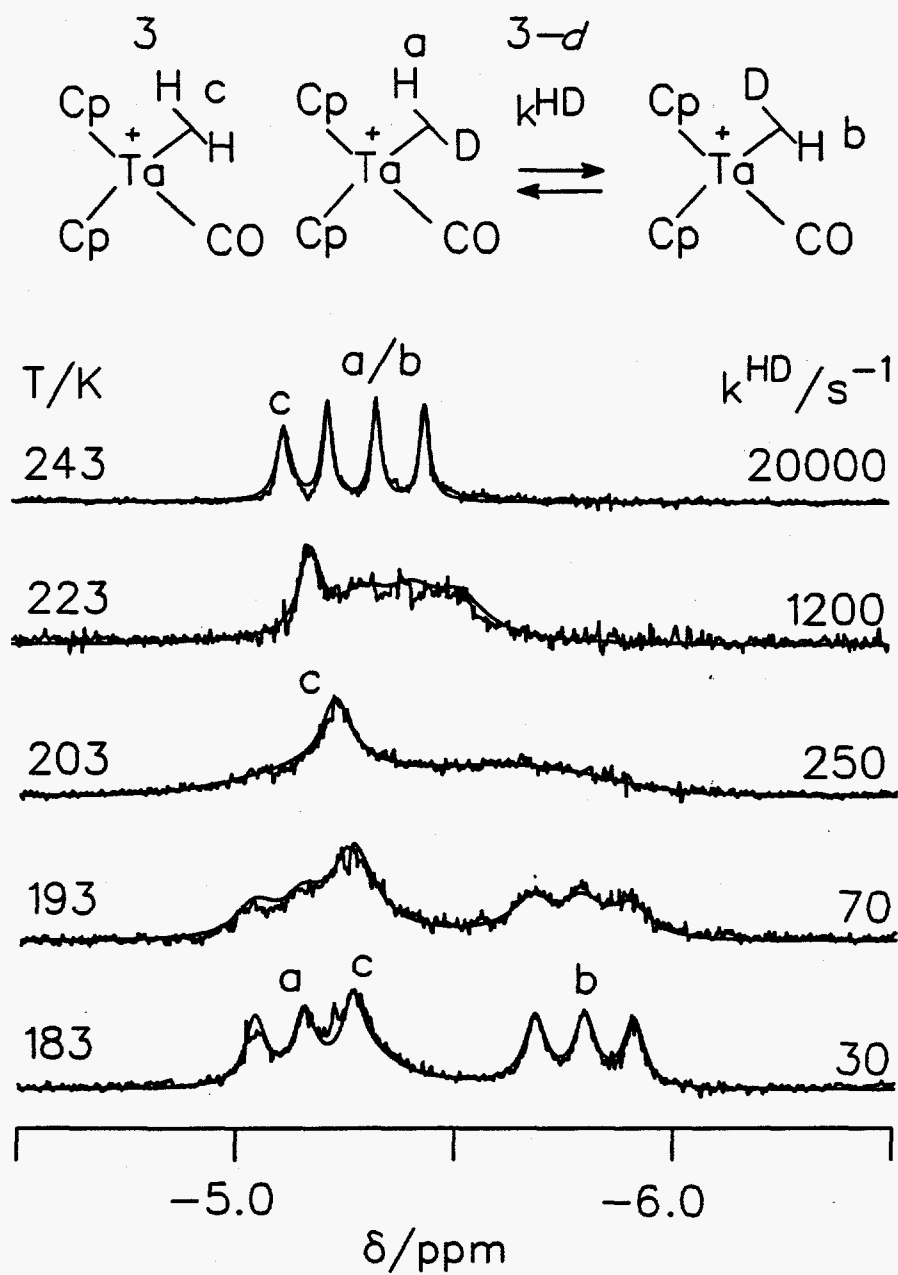Figure 5 Limbach et al.

Figure 6 Limbach et al.

Figure 7 Limbach et al.

Figure 8 Limbach et al.

$4 \quad (PCy_3)_2(CO)_3 W \!-\!\!\!\begin{array}{c} H \\ | \\ H \end{array}$

T/K

J/meV

W$_o$/meV

188   1.6   0.2

154   1.45   0.18

118   1.4   0.13

28.8   1.35   0.08

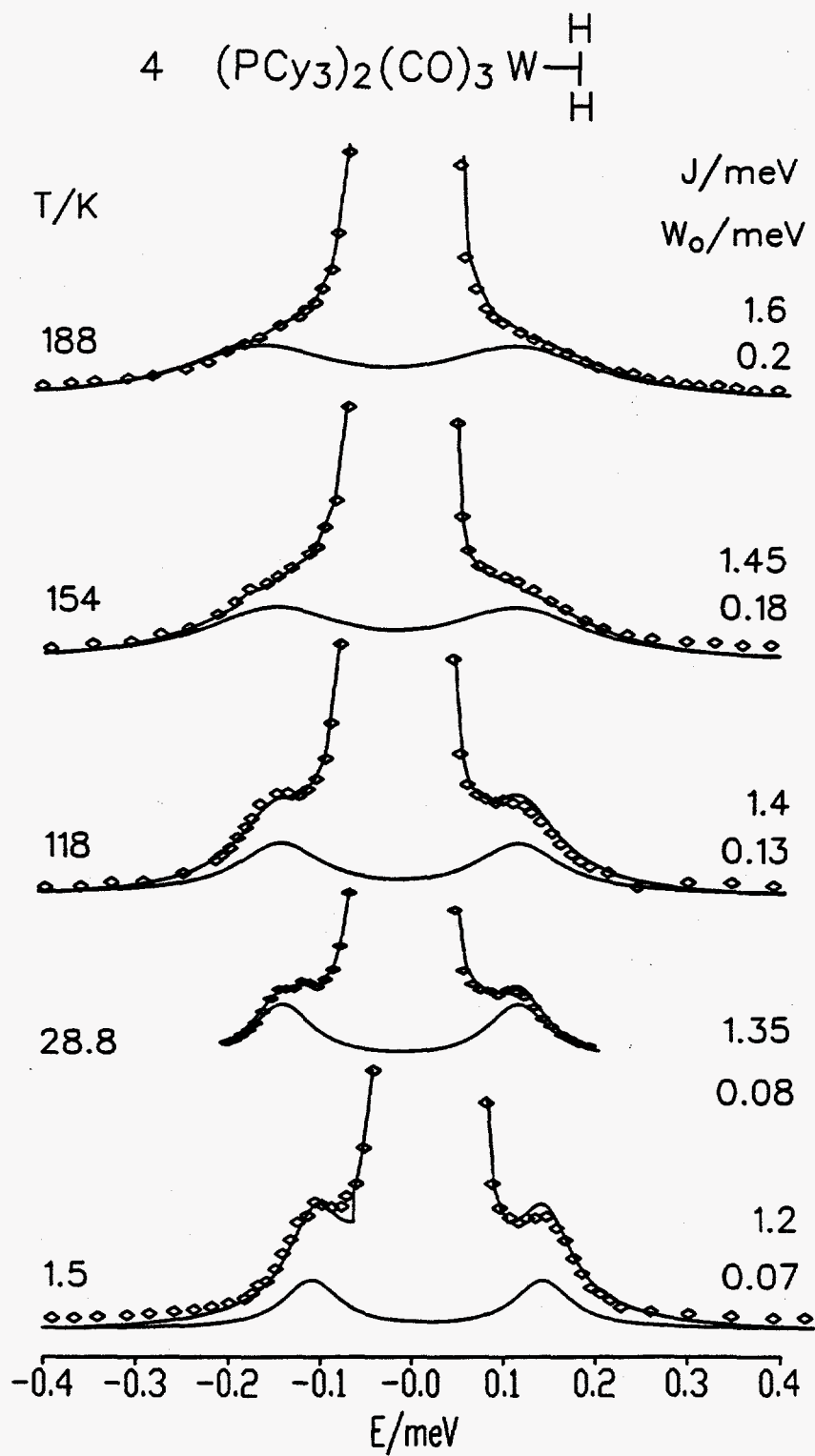1.5   1.2   0.07

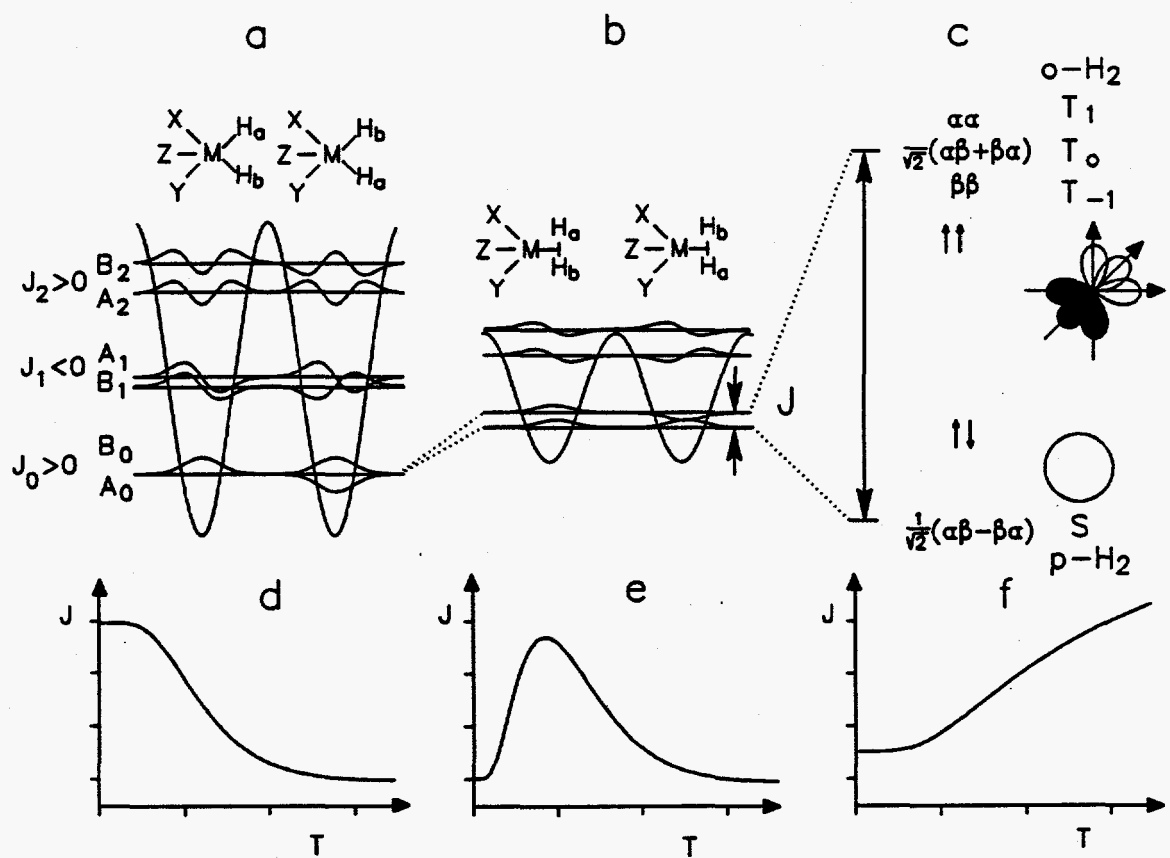-0.4   -0.3   -0.2   -0.1   -0.0   0.1   0.2   0.3   0.4

E/meV

Figure 9 Limbach et al.

Figure 10· Limbach et al.